E-cigarette exposure augments murine abdominal aortic aneurysm development: role of Chil1

Joscha Mulorz [1,2,3,4†], Joshua M. Spin[2,3,4†], Pireyatharsheny Mulorz[2,3,4†], Markus Udo Wagenhäuser[1], Alicia Deng[2,3,4], Karin Mattern[5], Yae H. Rhee[1,2,3,4], Kensuke Toyama[6], Matti Adam [7], Hubert Schelzig[1], Lars Maegdefessel[8,9,10], and Philip S. Tsao [2,3,4]*

[1]Clinic for Vascular and Endovascular Surgery, Medical Faculty and University Hospital Düsseldorf, Heinrich-Heine-University, Düsseldorf, Germany; [2]Department of Medicine, Stanford University, 300 Pasteur Drive, Standford, CA 94305, USA; [3]VA Palo Alto Health Care System, 3801 Miranda Ave, Palo Alto, CA 94304, USA; [4]Department of Medicine, Stanford Cardiovascular Institute, 300 Pasteur Drive, Standford, CA 94305, USA; [5]Department of Anesthesiology, Intensive Care and Emergency Medicine, Medical University of Göttingen, Göttingen, Germany; [6]Department of Pharmacology, Ehime University Graduate School of Medicine, Ehime, Japan; [7]Department of Cardiology, Heart Center, University of Cologne, Cologne, Germany; [8]Department for Vascular and Endovascular Surgery, Klinikum rechts der Isar, Technical University Munich, Munich, Germany; [9]Department of Medicine, Karolinska Institute, Stockholm, Sweden; and [10]German Center for Cardiovascular Research (DZHK), Berlin, Germany (partner site: Munich)

|	
Aims	Abdominal aortic aneurysm (AAA) is a common cardiovascular disease with a strong correlation to smoking, although underlying mechanisms have been minimally explored. Electronic cigarettes (e-cigs) have gained recent broad popularity and can deliver nicotine at comparable levels to tobacco cigarettes, but effects on AAA development are unknown.
Methods and results	We evaluated the impact of daily e-cig vaping with nicotine on AAA using two complementary murine models and found that exposure enhanced aneurysm development in both models and genders. E-cigs induced changes in key mediators of AAA development including cytokine chitinase-3-like protein 1 (CHI3L1/Chil1) and its targeting microRNA-24 (miR-24). We show that nicotine triggers inflammatory signalling and reactive oxygen species while modulating miR-24 and CHI3L1/Chil1 *in vitro* and that Chil1 is crucial to e-cig-augmented aneurysm formation using a knockout model.
Conclusions	In conclusion our work shows increased aneurysm formation along with augmented vascular inflammation in response to e-cig exposure with nicotine. Further, we identify Chil1 as a key mediator in this context. Our data raise concerns regarding the potentially harmful long-term effects of e-cig nicotine vaping.

---

* Corresponding author. Email: Tel: +1 650 493 5000 (x62991), ptsao@stanford.edu
† The first three authors contributed equally to the study.

Graphical Abstract
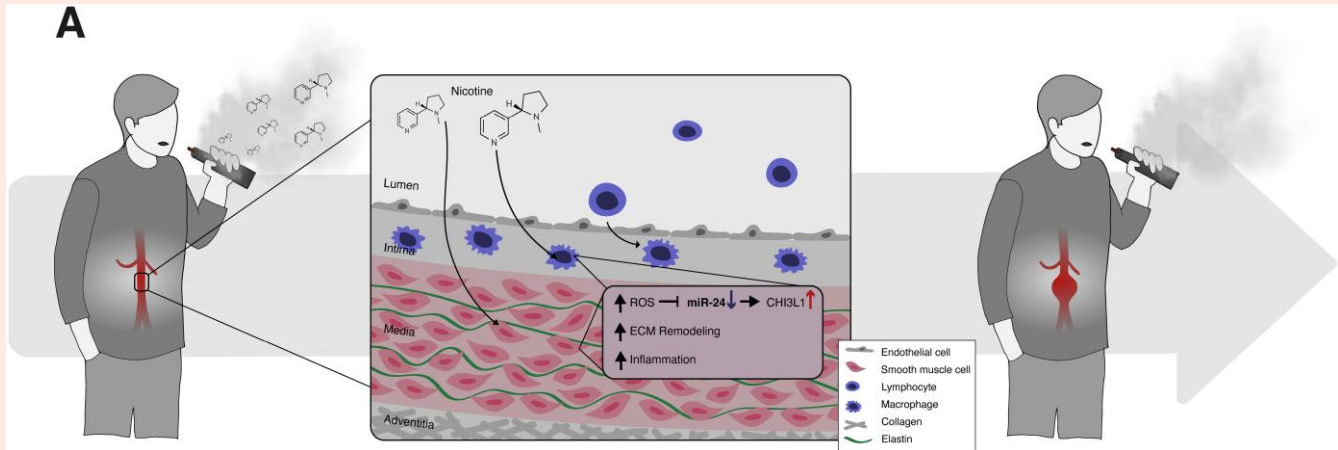
1. Introduction

Abdominal aortic aneurysms (AAA) cause significant morbidity and mortality. AAA prevalence remains high in recent reports,[1] and although improved endovascular and open surgical repair techniques have led to reduced mortality,[2] deaths due to ruptured AAA and its complications are still common.[3]

The most important known modifiable risk factor for AAA is a history of tobacco use. Only lung cancer displays a stronger disease association with smoking.[4] Over 90% of AAA patients relate a history of smoking,[5] and the augmenting effects of conventional cigarettes on AAA are well established from clinical trials and animal models.[6–10] Indeed, smoking cessation is a top clinical priority for AAA patients.[11] While traditional cigarette use has been declining in Western countries, alternative forms of nicotine delivery have become more common. Introduced in 2003, electronic cigarettes (e-cigs) and e-cig vaping have gained popularity as potentially 'healthier' substitutes for smoking, while still delivering nicotine at sufficient levels to satisfy addiction.[12]

Understanding the potential dangers of e-cigs has become increasingly urgent, as several recent studies have suggested elevated cardiovascular risk associated with their use.[13–15] Current e-cigs and similar devices release 'vapour' produced by heating a solution ('e-liquid' or 'e-juice'), usually containing nicotine as its active ingredient along with propylene glycol, glycerol, and sometimes flavouring chemicals.[16,17] While the health effects of inhaling e-cig vapour are not yet known in detail, it has been reported that vaping increases circulating levels of cotinine, the main nicotine metabolite, to comparable levels reached with tobacco cigarettes.[18] Importantly, no published study has addressed the potential effects of e-cigs in the context of AAA.

We and others have previously shown that subcutaneous infusion of nicotine accelerates expansion of AAA in murine models, in large part by affecting vascular smooth muscle cells (VSMC) and triggering inflammation.[19–21] Secondarily, we also found that chronic nicotine infusion induces murine aortic remodelling and regional vascular stiffness, elements predisposing to AAA.[22,23] However, these studies utilized continuous nicotine exposure, rather than repeated daily respiratory exposure.

MicroRNAs (miRs) are important regulators of transcriptional pathways,[24] and subcutaneous nicotine treatment has been shown to alter miR expression.[20,25,26] We have previously shown that miRs play a key role in aneurysm development, and can be modulated *in vivo*, thereby altering disease progression.[20,27–29] This suggests that e-cig vaping might also regulate cardiovascular miRs and influence AAA formation.

We now show for the first time that e-cig exposure (for purposes of this study, 'e-cig' refers to e-cig-generated vapour containing nicotine but no flavourings) affects murine vascular inflammation in the context of AAA development. We find that e-cigs accelerate experimental aneurysm progression and explore the mechanisms behind these effects *in vitro* and *in vivo*, with particular focus on the anti-inflammatory miR-24 and its target cytokine CHI3L1(human)/Chil1(mouse), a 18-glycosyl hydrolase family member. (Note that the human and murine orthologs have different names.)

We have previously shown that miR-24 directly modulates CHI3L1/Chil1 expression levels and through that mechanism can regulate cytokine synthesis, alter macrophage cell survival, and promote cytokine production and migration in aortic SMC.[29] CHI3L1 is an inflammatory biomarker candidate in cardiovascular disease. It has been found to be elevated in patients with coronary artery disease, with disease progression corresponding to augmented CHI3L1 levels.[30] Moreover, we observed that human AAA size correlated with higher CHI3L1 levels and that Chil1 expression increased during periods of murine model AAA growth.[29]

2. Methods

2.1 Mice

All animal protocols were approved by the Administrative Panel on Laboratory Animal Care at Stanford University (https://researchcompliance.stanford.edu/panels/aplac) and the VA Palo Alto Health Care System Institutional Animal Care and Use Committee (protocol # TSA1659) and followed the National Institutes of Health and U.S. Department of Agriculture Guidelines for Care and Use of Animals in Research. All experiments were performed with C57BL/6J (PPE model) and ApoE^tm1Unc (AngII model) mice. Animals were purchased from The Jackson Laboratory (Bar Harbor, ME, USA).

2.2 E-cig. vapour exposure

At 8 week-of age, C57BL/6J mice were exposed to e-cig vapour containing 50% propylene glycol, 50% vegetable glycerol, and 24 mg/mL nicotine for a total of 6 weeks using the SciReq InExpose system (SCIREQ, Montreal,

Canada). The exposure protocol included a puff duration of 9 s per minute, for a total of 60 min at the same time daily. The device used was a third-generation MOD e-cig (Shenzhen Joyetech Co., Shajing Town, China) with a temperature-controlled coil set to 230°C. Plasma cotinine levels were measured via ELISA according to the manufacture's protocol (Abcam, Cambridge, UK). Control animals were placed in SCIREQ chambers for the same daily duration but were exposed to room air only. The same protocol was applied to 8-week-old ApoE[tm1Unc] (i.e. ApoE^{−/−}) mice.

2.3 Porcine pancreatic elastase infusion model and angiotensin II model

The porcine pancreatic elastase (PPE) infusion model to induce mouse AAA was performed as previously described at 10 weeks of age.[31] The proximal and distal aorta were temporarily ligated or clamped, followed by an aortotomy above the iliac bifurcation. A catheter was used to infuse the aorta for 5 min at 120 mmHg with saline ('sham' surgery), or saline containing type I porcine pancreatic elastase (2.5 U/mL; Sigma Aldrich), and the aortotomy was then repaired. The induced AAA aortic segment (between the left renal artery and the bifurcation) was harvested at 7- or 28-days post-surgery.

For the AngII model, ApoE^{−/−} mice were implanted subcutaneously with osmotic mini pumps (Alzet, Model 2004) filled with either sterile saline or saline with angiotensin-II (1μg/kg/min, Sigma Aldrich) as previously described.[32]

Prior to surgery mice received sustained release buprenorphine (ZooPharm, Fort Collins, CO, USA) at 0.6–1.0 mg/kg subcutaneously and two drops of 0.25% bupivacaine solution (Hospira Inc., Lake Forest, IL, USA) locally. During surgery anesthesia was maintained with isoflurane 2.5%. Post-surgery, all animals received daily monitoring in accordance with the approved procedural protocols.

All mice were sacrificed with an inhalation overdose (5%) of isoflurane (Vet One, Meridian, ID, USA) and cervical dislocation or heart puncture followed by cervical dislocation. The aorta was transected and flushed via the left ventricle with ice cold phosphate buffered saline (PBS; pH 7.4). The aorta was then dissected from fat and connective tissue from the left renal artery to the bifurcation using a microscope (Leica, Wetzlar, Germany). Blood and aorta were snap-frozen individually in liquid nitrogen and stored at −80°C before further processing.

2.4 AAA growth and blood pressure monitoring

AAA development in both models was monitored via B-mode ultrasound (Vevo 2100® High-Resolution In Vivo Micro-Imaging System (VisualSonics, Toronto, Canada) at baseline and days 3, 7, 14, 21, and 28 post-surgery. Mice were studied under isoflurane anesthesia and aortic diameters were assessed at maximum diameter in the systolic cardiac phase. Non-operated C57BL/6J mice of each treatment group were also monitored for changes in blood pressure over a 4-week period using a non-invasive cuff-tail system (CODA non-invasive system, Kent Scientific Corporation, Torrington, USA), an established method reported to provide accurate blood pressure measurements over the physiological range of blood pressure in mice.[33]

2.5 Tamoxifen-inducible Chil1 knock-out

In Chil1 knock-out mice, the Chil1 gene exon 5 was flanked by two loxP sites generated by Applied StemCell, Inc. (Menlo Park, CA). Complete genomic knockout was verified by tail DNA polymerase chain reaction (PCR) using primers A1 5′- TAGACTCAGCCCCTGTGGTAATG −3′ (Chil1 genomic locus) and N1 5′- GTGTTGGTTTTTGTGTGCGGCG −3′ (targeting construct). The homozygotic Chil1 mice were then crossed to B6.Cg.Tg (UBC-Cre/ERT2)1EJb2J (Jax) to generate homozygous, systemic, conditional Chil1/Cre mice. Tamoxifen (Sigma-Aldrich) was dissolved in 100% corn oil (Sigma-Aldrich) at 20 mg/mL and injected intraperitoneally at 75 mg/kg for five consecutive days at the age of 7 weeks. DNA PCR

confirmed effective knockout in tail and aorta using the above primers. Knockout of full Chil1 transcript in aortic tissue was further confirmed by Taqman real-time quantitative reverse transcription polymerase chain reaction (qRT-PCR) (Life Technologies, Mm00801477_m1, probe covers exon 6–7 boundary) which showed the transcript was undetectable.

2.6 Histologic assessment

For histological staining, aortic tissue was obtained and prepared for frozen sectioning as previously described.[20,29] Sectioning, staining and IHC were performed by Histotec (Histotec, Fremont, CA, USA). Antibodies were obtained from Cell Signaling Technology, Danvers, Massachusetts, USA (#70076S for F4/80, dilution 1:250; and #47066S for Chil1, dilution 1:250). The automated quantification of Chil1- and F4/80-positive areas was performed using Fiji software.[34] All histological images were obtained at room temperature using a Keyence Microscope (Model BZ-X810, Keyence) with built-in Nikon CFI 60 Series infinite optical system (Nikon).

2.7 RNA quantification

Total RNA was isolated using a TRIzol-based (Invitrogen) RNA isolation protocol. RNA was quantified by Nanodrop (Agilent Technologies), and RNA and miRNA quality were verified using an Agilent 2100 Bioanalyzer (Agilent Technologies). Samples required 260/280 ratios >1.8, and sample RNA integrity numbers ≥9 for inclusion. RNA was reverse transcribed using the TaqMan microRNA Reverse Transcription kit (Thermo Fisher) according to the manufacturer's instructions. MicroRNA and TaqMan assay kits (Thermo Fisher) for miR-24, sno202 (endogenous control for normalization in mice), and RNU44/48 (control for human samples) were used.

For mRNA, the VILO cDNA synthesis kit (Thermo Fisher) was used to synthesize first-strand cDNA according to the manufacturer's protocol. TaqMan qRT–PCR assays were performed using mouse- and human-specific primers (Thermo Fisher). Relative expression of miR-24-1 and miR-24-2 was obtained by TaqMan for human and murine pri-miR-24-1 and pri-miR-24-2 (Thermo Fisher). All probes were normalized to 18S as a multiplexed internal control. Amplification took place on a QuantStudio12K Flex (Thermo Fisher). All fold changes were calculated by the method of ΔΔCt, and are expressed as mean ± SEM compared to either sham-operated mice, saline-infused mice, or control-treated cells (in vitro). All experiments included 5–12 samples per group and time point.

2.8 In vitro studies

Human aortic smooth muscle cells (AoSMC) were propagated in growth media [SmGM-2 (for AoSMC) with 5% fetal bovine serum (FBS) per standard protocols (Lonza; passage #4–5)]. AoSMC were incubated in basal medium (SmBM) for 48–72 h prior to treatment/transfection. RAW264.7 cells (ATCC) were employed as a cell model surrogate for murine macrophages, and propagated in DMEM + 10% FBS per manufacturer's instructions. Cells were treated with human or murine recombinant IL-6 (20 ng/mL) (Cell Signaling) and/or liquid nicotine (10 nM or 100 nM, #N3876, Sigma-Aldrich, St. Louis, Missouri, USA) for 24 h. Cells were harvested for RNA analysis at approximately 90% confluence. We performed ROS assays with rhodamine in AoSMC (Abcam/ab139476) using pyocyanin (300 μM) as a positive control given 30 min prior (or untreated), and then treating with nicotine with or without IL-6 for 1 h. Measurements were taken according to the manufacturer's instructions. The DCFDA Cellular Reactive Oxygen Species (ROS) Detection Assay Kit (Abcam/ab113851) was used to quantitatively measure ROS in adherent RAW264.7 cells after 24 h of treatment. Cells were treated with either 10 nM or 100 nM nicotine (Sigma-Aldrich) and 500 nM TEMPOL (4-Hydroxy-TEMPO, Sigma-Aldrich) and measured according to the manufacturer's instructions using a microplate reader.

2.9 Transfection of cultured cells

Transfection of AoSMC was performed using Lipofectamine RNAiMAX (Thermo Fisher) reagent, mixed with anti-hsa-miR-24, pre-hsa-miR-24 or scrambled controls (Thermo Fisher).[29] For each transfection, scr-,

anti- or pre-miR (final transfection concentration: 50 nM) was diluted in Opti-MEM (Gibco) and combined with RNAiMAX per manufacturer's protocol. Two hours after transfection, cells were treated with IL-6 and/or nicotine as described above and harvested 24 h later. RNA was extracted using TRIzol (Invitrogen). Some experiments utilized simultaneous transfection with 50 nM siRNA directed against CHI3L1, with negative siRNA controls (Thermo Fisher), as previously described.[29]

2.10 Regulation of miR-24 through nf-κB by nicotine in vitro

Transfection of IL-6-treated RAW264.7 cells was performed using Lipofectamine RNAiMAX (Invitrogen) reagent, and siRNA targeting Rela (p65) subunits of the transcription factor NF-κB (Thermo Fisher). For each transfection, siRNA was diluted in Opti-MEM (Gibco) for a final transfection concentration of 50 nM. Cells were transfected with Lipofectamine/siRNA 6 h prior to treatment with IL-6 (20 ng/mL) and/or nicotine and incubated for an additional 24 h, followed by harvest and RNA extraction using TRIzol (Invitrogen). Successful knockdown (>75%) was confirmed by qRT–PCR determining expression levels of Rela (p65) as well as decreased nuclear NF-κB activity (ELISA; Active Motif, Carlsbad, CA, USA) in control-siRNA- and siRela-treated cells.

2.11 Human tissue sample acquisition and preparation

Human aortic tissue samples were obtained from the Karolinska University Hospital Biobank in Solna and were derived from patients who underwent surgical repair of their AAA. These samples were obtained from a matched cohort of patients with and without a history of active smoking. Approval for studies on human tissue samples were obtained under informed consent complying with all guidelines and policies of the Stanford University School of Medicine and the Karolinska Institute, in accordance with the Declaration of Helsinki.

2.12 Statistics

Data are presented as mean ± SEM. Groups were compared using Student's *t*-test (two-tailed) for parametric data. When comparing multiple groups, data were analyzed by ANOVA with Bonferroni's post-test. Sequential measurements were analyzed by One-Way Repeated Measures ANOVA. Paired *t*-testing was performed utilizing Wilcoxon matched-pairs signed rank test with Spearman effectiveness testing. Aortic diameters were compared using two-way ANOVA (α 0.05) with multiple comparisons. All statistic testing and graph composition was done using GraphPad Prism software (San Diego, USA). A value of $P \leq 0.05$ was considered statistically significant.

3. Results

3.1 E-cig vaping exacerbates experimental murine aneurysm development and augments the miR-24/Chil1 response

Eight-week-old C57BL/6J mice of both genders were exposed to daily e-cig vapour (or room-air control) for 6 weeks. After 2 weeks of exposure for preconditioning and familiarization, AAA was surgically induced in the infrarenal segment with PPE infusion (or saline for sham-operation) (*Figure 1A*) and aortic dilation was monitored using ultrasound (Supplementary material online, *Figure S1A*). E-cig exposure did not significantly alter blood pressure or weight in C57BL/6J mice (Supplementary material online, *Figure S1B and C*). Sufficient nicotine uptake through vaping was ensured by measuring cotinine levels in serum (Supplementary material online, *Figure S1D*). Cotinine levels obtained were consistent with levels found in humans with moderate-heavy smoking or e-cig vaping.[35]

In-vivo ultrasound monitoring demonstrated that male mice in the e-cig group developed larger AAA when compared to mice exposed to room air after PPE infusion. As expected, sham surgery with intra-aortic saline infusion did not lead to AAA development; e-cig exposure alone (with sham surgery) also did not lead to AAA development (*Figure 1B*). Similar effects were observed in female mice undergoing PPE surgery which also developed larger lesions when exposed to e-cig, while sham surgery did not lead to significant changes in aortic diameters (Supplementary material online, *Figure S1E*).

Selected mice were euthanized at either 7 or 28 days after surgery to harvest the aneurysmal (or equivalent control) region of the aorta for RNA extraction. Quantitative RT–PCR confirmed that expression of pro-inflammatory (*Il6, Ccl2*) and extracellular matrix (ECM) remodelling genes (*Mmp9*) known to be crucial for AAA development were increased in mice exposed to e-cig (vs. room air) by 7 days after surgery, while elastin (*Eln*) showed further decreased expression (*Figure 1C*). E-cig exposure also led to a mildly enhanced inflammatory response in non-aneurysmal tissue, though to a much lesser extent than with AAA. These findings were sustained throughout the observation period (28 days) for pro-inflammatory genes and to some extent also for genes essential for ECM-remodelling (*Figure 1C*). In female PPE-induced AAA, similar observations were made for both time points when comparing e-cig-exposed mice to room air exposure and to sham surgery (Supplementary material online, *Figure S2A and B*).

Of note, aortic expression of the novel cytokine *Chil1* was significantly upregulated in mice of both genders exposed to e-cig (vs. room-air controls with or without PPE or sham surgery) at both early and later time points, and was regulated in the opposite direction from miR-24 expression (*Figure 1D and E*; Supplementary material online, *Figure S2C*). In previous work sampling murine PPE-AAA tissue, miR-24 (an anti-inflammatory miR) was also noted to be down-regulated, and displayed the most significant negative correlation with upregulated target genes at Day 7 of any individual down-regulated miRNA (by miRNA-target seed-hexamer enrichment using DIANA-mirExTra).[29]

PPE induction of AAA in male animals exposed to room-air led to significant, but more limited upregulation of Chil1 (with similar opposing miR-24 regulation) when compared to e-cig-exposed mice (*Figure 1D and E*). Again, similar regulatory patterns were observed in female mice (Supplementary material online, *Figure S2C*).

Immunohistochemical analysis demonstrated enhanced Chil1 protein expression in AAA tissue after 28 days (*Figure 1F and G*). We also observed increased F4/80 marker expression in the aneurysms of e-cig-exposed (vs. room air) animals after 28 days, indicating enhanced macrophage infiltration when mice were exposed to e-cig vapour (*Figure 1F and G*).

The same e-cig vaping protocol was applied to male ApoE$^{-/-}$ mice receiving osmotic mini pumps containing Angiotensin-II (AngII) to induce dissecting AAA in the suprarenal aortic segment. Again, aortic growth was monitored for 28 days via ultrasound. As often occurs with this model, female mice did not develop AAA at sufficient rates or diameters for comparative analysis. However, in male mice e-cig exposure again led to augmentation of aneurysm growth (*Figure 1H*), and both significant aortic miR-24 down-regulation, and up-regulation of *Chil1* expression (*Figure 1I*) when compared to room air-exposed mice. The e-cig group also revealed increased Day 28 inflammatory gene expression (*Il6, Ccl2*) and augmented regulation of ECM remodelling genes (*Mmp2, Mmp9, Eln*) when compared to room-air (Supplementary material online, *Figure S3A*).

3.2 Nicotine increases inflammatory gene expression in AAA-related cell types in vitro

We sought to identify the specific effects of nicotine treatment on inflammatory gene expression in cell subtypes known to be crucial for AAA, including macrophages and aortic smooth muscle cells.

Nicotine treatment significantly increased expression levels (by qRT–PCR) of pro-inflammatory genes in RAW264.7 murine macrophages (*Figure 2A*). Further, nicotine dose-dependently augmented pro-inflammatory responses
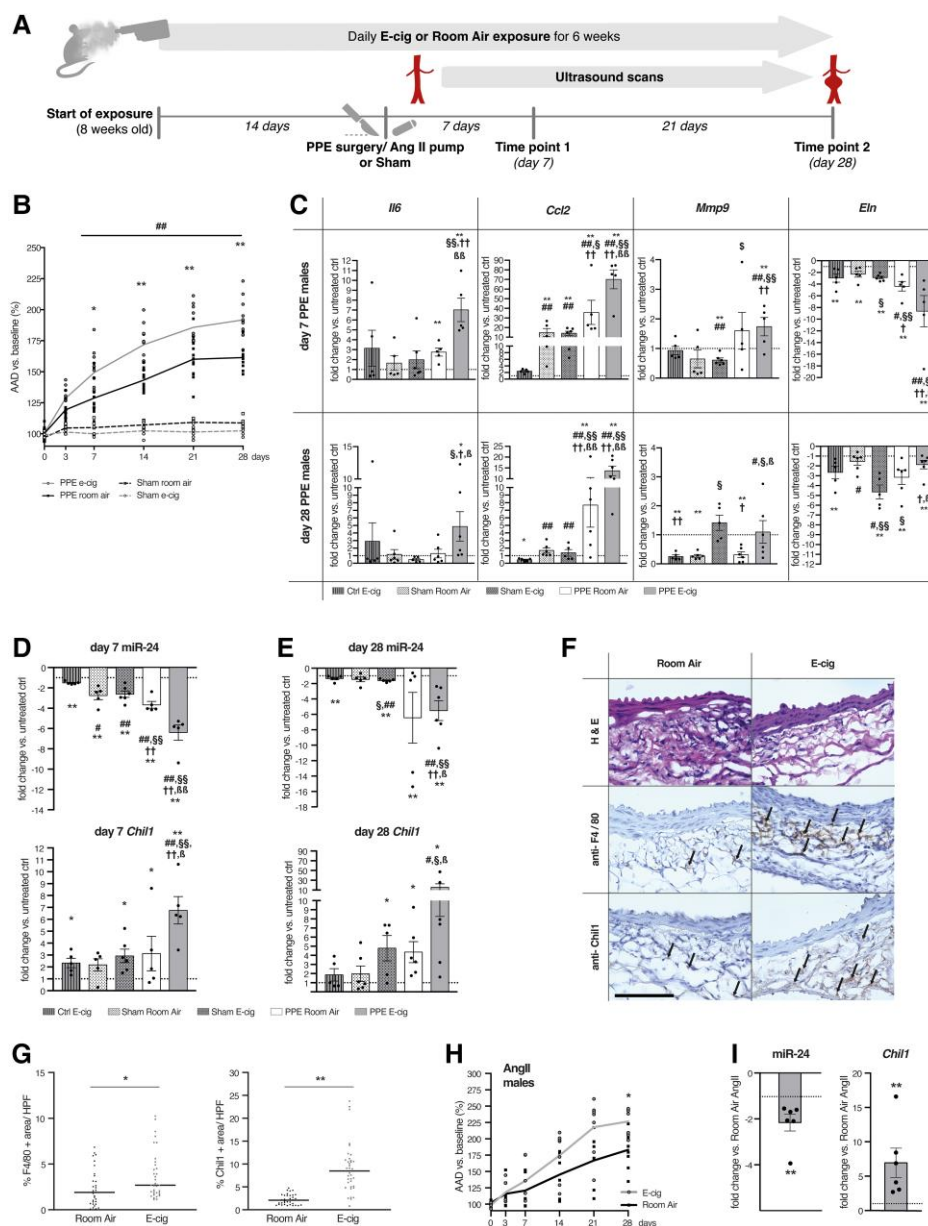
Figure 1 AAA progression and gene expression, miR-24, and *Chil1* response to E-cig exposure during AAA development. (*A*) Schematic timeline of E-cig vaping experiments. Aortic ultrasound scans were performed at baseline, at day 3 and day 7 after AAA induction, and then weekly. (*B*) Daily exposure to E-cig in male C57BL/6J mice containing nicotine (24 mg/mL, 9 s puffs per minute, 60 min/d) increased AAA diameter by ultrasound vs. Room air-exposed control animals after PPE and vs. sham surgery with or without E-cig (*n* = 5-13 per group). Sham surgery did not lead to aortic dilation in E-cig or room air-exposed animals. (*C*) Gene expression of key inflammatory markers (*Il6*, *Ccl2*) and ECM-related genes (*Mmp9*, *Eln*) (*n* = 5–6 per group) in males at day 7 (top) and day 28 (bottom) in aortic tissue derived from untreated animals, or after sham or PPE surgery with or without E-cig exposure. (*D* and *E*) Gene expression of miR-24 and its target *Chil1* in the same tissues as in *C* quantified by qRT–PCR at day 7 (*D* left) and 28 (*E* right) (*n* = 5–6 per group). (*F*) Aortic aneurysm sections from male animals were harvested after 28 days and stained with hematoxylin and eosin, and IHC was used for anti-F4/80 and anti-Chil1. Positive areas were quantified. Scale bar is 100 μm. Arrows indicate positively stained areas. (*G*) IHC of F4/80- (top) and Chil1- (bottom) positive areas were quantified in high power fields (HPF) (4 HPF per slide, 3 slides per animal, 3 AAA per group). (*H*) Male ApoE$^{-/-}$ mice were exposed to E-cig according to the same protocol as used in *A*. After 2 weeks of pre-exposure to E-cig or Room-air, osmotic minipumps filled with Ang-II were implanted and suprarenal aortic growth was measured via ultrasound (*n* = 8 per group). (*I*) miR-24 and *Chil1* gene expression levels in AAA tissues from E-cig-exposed (vs. Room-air-exposed, Ang-II-treated-) ApoE$^{-/-}$ mice using qRT–PCR at Day 28 after pump implantation (*n* = 5–6 per group). Graphs (*B* and *H*) show aortic aneurysm diameter (AAD) % increase vs. baseline. *$P < 0.05$; **$P < 0.01$ AAA E-cig vs. AAA room air. ##$P < 0.01$ both PPE groups vs. both sham surgery groups. All by two-way ANOVA with multiple comparison (*B* and *H*). Gene expression data are presented as fold change (FC) vs. unoperated, room air-exposed control. *$P < 0.05$ or **$P < 0.01$ vs. Sham; #$P < 0.05$ or ##$P < 0.01$ vs. unoperated, e-cig-exposed control; §$P < 0.05$ or §§$P < 0.01$ vs. sham-operated, room air-exposed control; †$P < 0.05$ or ††$P < 0.01$ vs. sham-operated, e-cig-exposed control; ß$P < 0.05$ or ßß$P < 0.01$ vs. PPE-operated, room air-exposed. Two tailed student's *t*-test (*C*, *D*, *E*, and *I*). *$P < 0.05$; **$P < 0.01$ Two tailed student's *t*-test (*G*) Data are mean ± SEM. Down-regulated genes are shown as −1/FC.
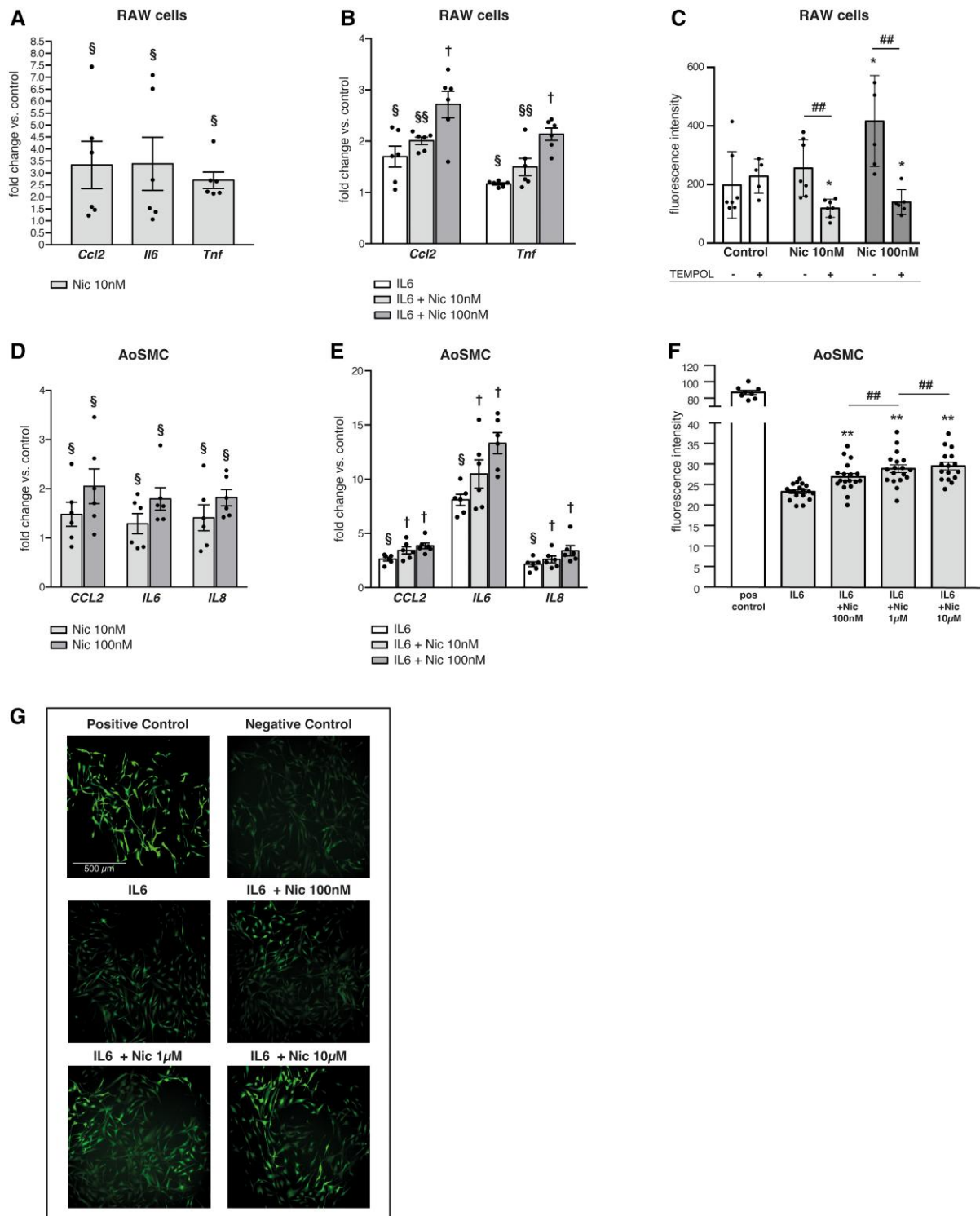
Figure 2 Nicotine induces and augments pro-inflammatory cytokines and ROS in human AoSMC and murine RAW264.7 cells. (*A*) Nicotine increases expression levels of inflammatory genes (*Ccl2*, *Il6* and *Tnf*) in murine RAW264.7 cells. (*B*) Nicotine dose-dependently augments inflammatory gene (*Ccl2*, *Tnf*) responses to recombinant IL-6 treatment (20 ng/mL) in RAW264.7 cells. (*C*) Nicotine dose-dependently increases total ROS in RAW264.7 cells (DCFDA Assay, Ex/Em = 485/535 nm), a process reversed by TEMPOL. (*D*) Nicotine dose-dependently increases expression levels of inflammatory genes (*CCL2*, *IL6* and *IL8*) in human AoSMCs. (*E*) Nicotine dose-dependently augments inflammatory gene (*CCL2*, *IL6* and *IL8*) responses to recombinant IL-6 treatment (20 ng/mL) in human AoSMCs. (*F*) Nicotine dose-dependently increases ROS response to IL6 (20 ng/mL) in human AoSMCs (Abcam/Rhodamine, Ex/Em = 550/620 nm). (*G*) Corresponding pictures to (*F*) of human AoSMCs stained for ROS under green channel using ROS Detection Assay (Abcam/Rhodamine). Gene expression data are qRT–PCR presented as fold change vs. control. §$P < 0.05$ vs. control; vs. §§ control and IL6; † vs. control, IL6, and IL6 + nicotine 10 nM (*A*, *B*, *D*, and *E*). *$P < 0.05$ vs. control; #$P < 0.05$ vs. other group (*C*). *$P < 0.05$ or **$P < 0.01$ vs. IL6, #$P < 0.05$ vs. other group (*F*). All two-tailed Student's *t*-test. Data are mean ± SEM ($n = 4$–6/treatment group).
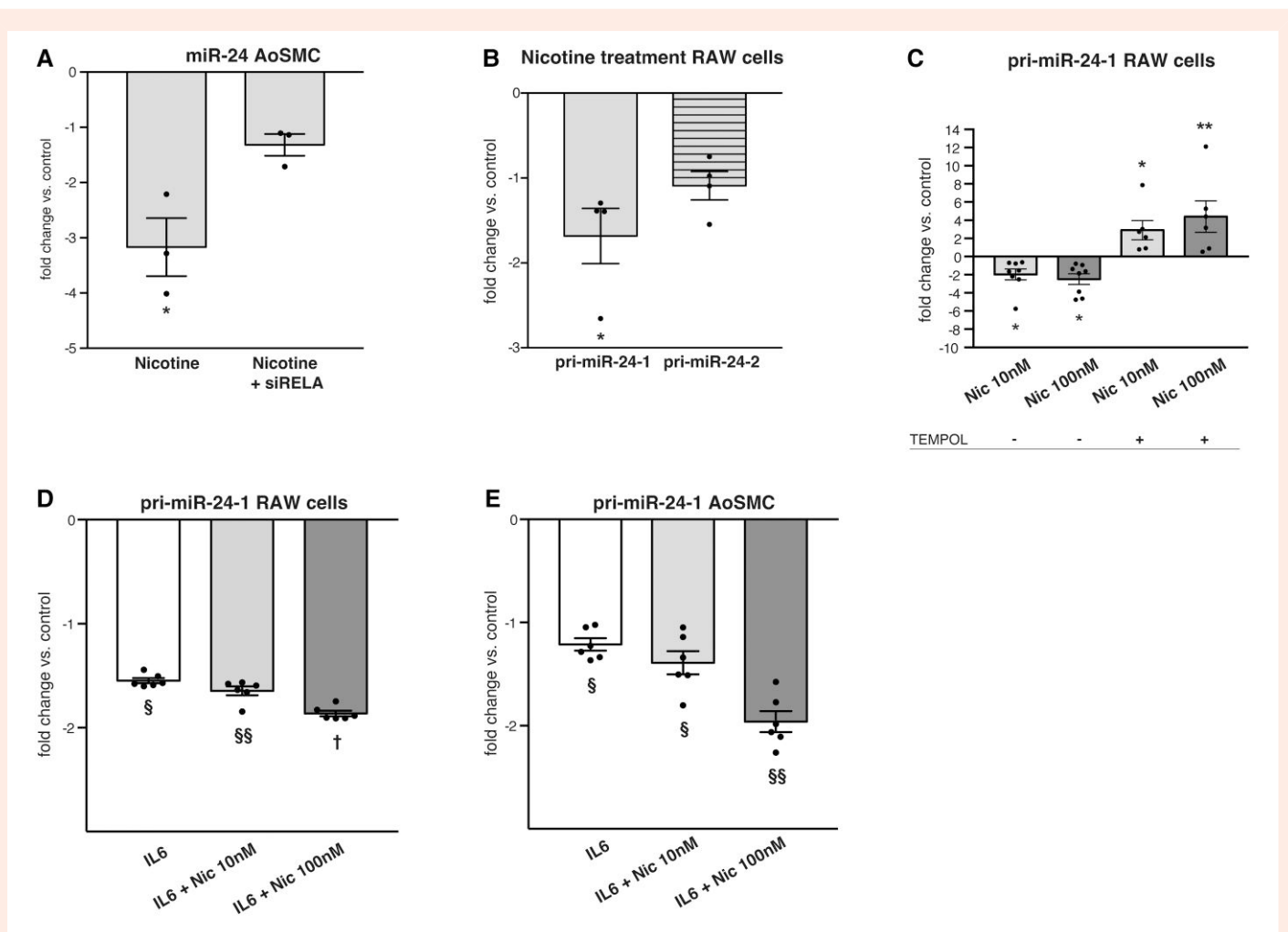
Figure 3 Nicotine down-regulates miR-24-1. (*A*) Nicotine (10 nM) down-regulates miR-24 expression in human AoSMCs via the NF-kB pathway. Down-regulation is neutralized with siRNA to RELA. (*B*) Nicotine (10 nM) down-regulates pri-miR-24-1 but not pri-miR-24-2 in RAW264.7 cells. (*C*) Nicotine reduces pri-miR-24-1 expression in RAW264.7 cells via ROS. Addition of ROS-scavenger TEMPOL leads to an increase in pri-miR-24-1 expression despite nicotine treatment. (*D* and *E*) Recombinant IL-6 treatment lowers pri-miR-24-1 in RAW264.7 cells and human AoSMCs, a process which is augmented dose-dependently by nicotine. Gene expression data are presented as fold change vs. control. *$P < 0.05$ vs. untreated control (*A*, *B*, and *C*). §$P < 0.05$ vs. control; §§ vs. control and IL6; † vs. control, IL6, and IL6 + Nic10 nM (*D* and *E*). All Student's *t*-test. Data are mean ± SEM ($n = 3$–8/treatment group). Down-regulated genes are shown as −1/FC.

in these cells when they were pre-treated with IL-6, one of the most prominent cytokines involved in AAA formation (*Figure 2B*).

ROS represent a class of signalling molecules that can mediate a multitude of processes, including NF-kB activation and vascular inflammation, and are key mediators in AAA progression.[36] Nicotine induces ROS in various cell types in culture as well as in aortic wall in murine AAA,[37] a process that has been invoked as a mechanism through which smoking might induce AAA. In RAW264.7 cells, we observed that nicotine treatment induced total ROS with increasing dose. This was negated by co-treatment with the ROS scavenger, TEMPOL (*Figure 2C*). Similar effects were found in primary human aortic smooth muscle cells (AoSMC): nicotine treatment significantly increased *CCL2, IL6* and *IL8* gene expression (*Figure 2D*). Futhermore, nicotine dose-dependently augmented inflammatory gene expression in AoSMCs induced by recombinant human IL6 pretreatment (*Figure 2E*). Importantly, we found that AoSMCs also showed increased total ROS production (*Figure 2F and G*; Supplementary material online, *Figure S3B*) in response to nicotine after IL-6 pre-treatment.

3.3 Nicotine regulates miR-24-1 and CHI3L1/Chil1 in aneurysm-related cells

In vitro stimulation of human AoSMC with nicotine significantly decreased miR-24 expression. This process appeared to be largely dependent upon NF-κB activation, as prior transfection with siRNA directed against RELA nearly eliminated the effect when compared with negative control transfection (*Figure 3A*).

MiR-24 transcription occurs at two loci in both the mouse and human genomes, and the products of each locus are subsequently processed to mature miR-24. Our previous[29] and current expression data indicate that pri-miR-24-1 (rather than pri-miR-24-2) is preferentially reduced in experimental AAA. We further investigated this in RAW264.7 cells, finding that nicotine treatment suppressed pri-miR-24-1 expression, but not pri-miR-24-2 (*Figure 3B*). This effect was mediated by ROS, as TEMPOL treatment prevented nicotine-induced pri-miR-24-1 down-regulation (*Figure 3C*). Additionally, nicotine exacerbated the downregulation of pri-miR-24-1 transcription induced by recombinant murine IL6
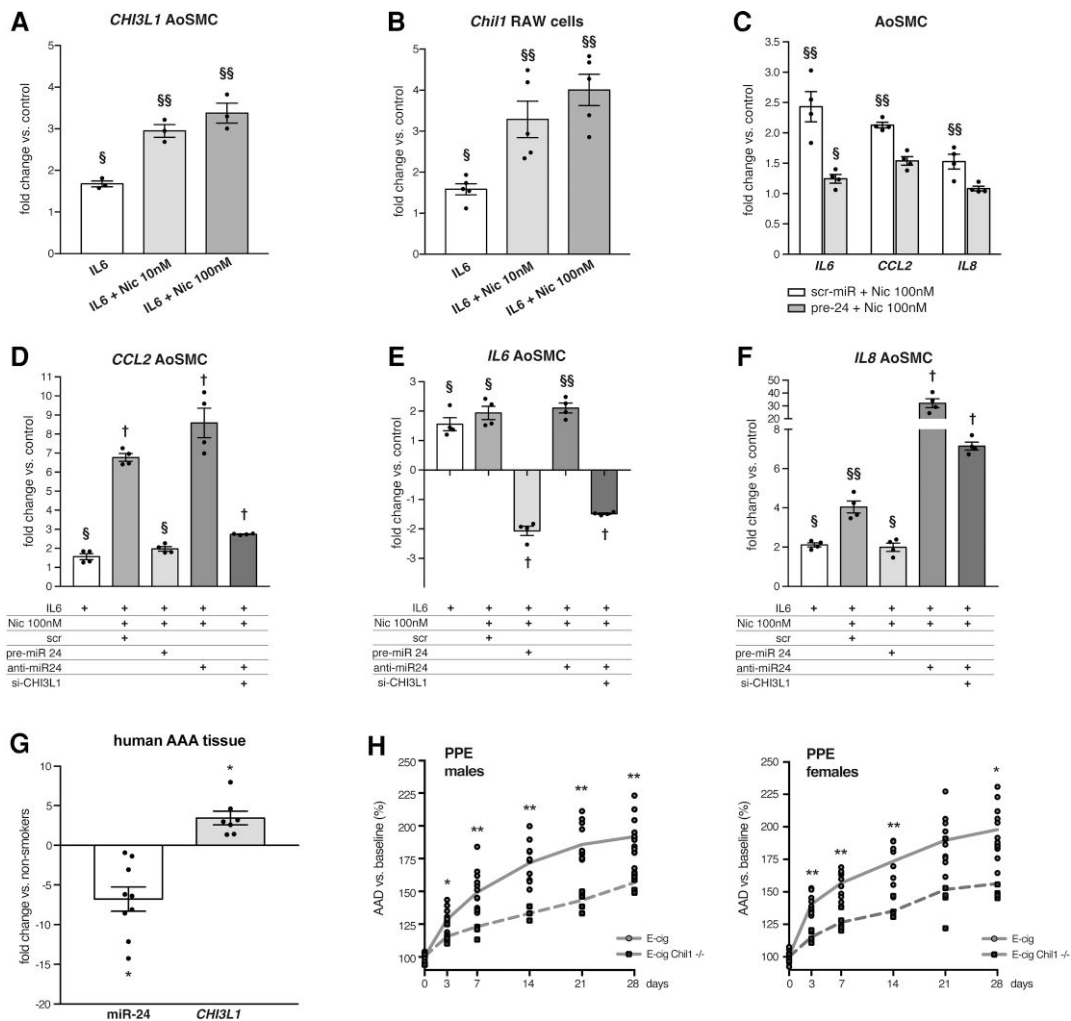
Figure 4 Nicotine-induced CHI3L1/Chil1 is crucial to the augmentation of both the inflammatory response and AAA development. (*A* and *B*) Nicotine augments IL6-induced increase of *CHI3L1/Chil1* gene expression in human AoSMCs and RAW264.7 cells by qRT–PCR. (*C*) Overexpression of miR-24 using transfection with pre-miR-24 (pre-24) reduces nicotine-augmented cytokine (IL6, CCL2 and IL8) gene expression in human AoSMCs. Scr-miR = scrambled miR control. (*D–F*) Nicotine augments the effects of IL6 in increasing inflammatory cytokines *CCL2* (*D*), *IL6* (*E*), and *IL8* (*F*) gene expression in human AoSMCs. These effects are reduced or reversed with miR-24 overexpression (pre-miR-24 transfection). Conversely, further down-regulation of miR-24 with anti-miR-24 transfection augmented the effects on inflammatory gene expression. However, simultaneous silencing of CHI3L1 (siRNA transfection) reduces or reverses the effects of the combination of IL6, nicotine and anti-miR-24. (*G*) Smoking augments the increase in aortic CHI3L1 gene expression, and the decrease in miR-24 in human AAA tissue ($n = 6$–9 per cohort). (*H*) Globally induced Chil1$^{-/-}$ suppresses AAA growth after PPE surgery in male (left) and female mice (right) exposed to E-cig vapour for a total of 6 weeks ($n = 5$–13 for males; 5–10 for females). Gene expression qRT–PCR data are presented as fold change vs. control. §$P < 0.05$ vs. control; vs. §§ control and IL6; † vs. control, IL6, and IL6 + Nic10 nM (*A–F*), two-tailed student's *t*-test, data are mean ± SEM ($n = 3$–6/treatment group). *$P < 0.05$ two-tailed Student's *t*-test (*G*). Down-regulated genes are shown as −1/FC. Graphs show aortic aneurysm diameter (AAD) % increase vs. baseline. *$P < 0.05$ or **$P < 0.01$ in two-way ANOVA with multiple comparison (*H*).

(*Figure 3D*). Similar findings were observed in human AoSMCs (*Figure 3E*). These observed effects of nicotine upon miR-24-1 were accompanied by dose-dependently increased expression of *CHI3L1/Chil1* in both human AoSMCs and RAW264.7 cells (*Figure 4A and B*).

3.4 Nicotine-induced increases in inflammatory genes are mediated in part by miR-24 and CHI3L1

As noted above, serum-starved human AoSMCs stimulated with recombinant IL-6 show additional increases in gene expression of inflammatory cytokines when treated with nicotine. These effects were largely neutralized when cells were transfected with pre-miR-24 (*Figure 4C*). SiRNA directed against CHI3L1 was able to abrogate the majority of the combined pro-inflammatory effects of anti-miR-24, IL6 and nicotine. Even in the presence of recombinant IL-6, pre-miR-24 was able to offset the cytokine increases seen in nicotine-treated human AoSMCs (vs. scrambled miR) (*Figure 4D–F*). Notably, the addition of anti-miR-24 significantly increased *IL8* expression beyond that achieved with IL-6 and nicotine together (*Figure 4F*). These data suggest that the miR-24/CHI3L1 axis is responsible in part for nicotine's additive inflammatory effects.

3.5 miR-24 and CHI3L1 show augmented regulation in AAA tissue from smokers

Given that e-cigs are fairly new products, the availability of human AAA samples from patients using e-cig devices is limited. To test whether chronic nicotine exposure affects CHI3L1 and its regulator miR-24 in human AAA disease, we investigated whether conventional cigarette smoking status affected relative levels of CHI3L1 and miR-24 in human AAA samples. Intriguingly, we found that active smokers showed significantly more regulation, with 4.98-fold greater down-regulation of miR-24, and 3.51-fold greater up-regulation of *CHI3L1* ($P < 0.05$, $n = 6–9$ in each cohort) (*Figure 4G*). Supporting clinical information is provided in the supplemental data (Supplementary material online, *Figure S3C*).

3.6 Role of Chil1 in e-cig-augmented AAA development

We further investigated the role of Chil1 in the context of e-cig exposure in AAA by applying the same vaping and PPE surgery protocols described above to age-matched mice of both genders after conditional knockout of *Chil1* in C57BL/6J mice. Knock-out efficiency was verified by PCR (Supplementary material online, *Figure S4A*). Accelerated AAA formation after e-cig exposure was significantly reduced in Chil1$^{-/-}$ mice (*Figure 4H*). This effect was apparent in both male and female mice. Notably, tamoxifen pre-treatment of wildtype mice at the same doses used for knock-out induction did not lead to changes in AAA growth (Supplementary material online, *Figure S4B*). Chil1$^{-/-}$ mice exposed to only room air did not show reduced AAA formation when compared to room air-exposed wildtype mice (C57BL/6J) AAA (Supplementary material online, *Figure S4C*).

4. Discussion

In the present study, we demonstrate for the first time that episodic inhaled e-cig vapour augments experimental AAA. We also identified a key mechanism behind the e-cig effects involving the cytokine Chil1 (also implicating its targeting regulator: miR-24), and further demonstrate the importance of nicotine's role in AAA formation.

While tobacco smoking is well-established as a major risk factor for cardiovascular disease in general, and AAA in particular,[5,6,9,38] less attention has been paid to the specific cardiovascular risks that may be due specifically to nicotine, a major constituent of both tobacco smoke and e-cigs. Nicotine is the major active ingredient in most e-liquids, in concentrations comparable to, or even higher than those found in conventional cigarettes.[18]

Chronically infused nicotine has been shown to augment aortic AAA progression in animal models, including with AngII-infusion in ApoE$^{-/-}$ mice and in the PPE model in C57BL/6J mice.[20] Wang et al. have also reported that infused nicotine can induce AAA formation in ApoE$^{-/-}$ mice.[21] However, all previously published experimental AAA studies employing nicotine have utilized direct continuous subcutaneous delivery, leaving it unclear how episodic daily uptake through the respiratory system might alter that response.

In the current study, we exposed mice to e-cig vapour containing nicotine to evaluate for the first time the impact on murine AAA development, using both the PPE and the AngII/ApoE$^{-/-}$ models. We chose a nicotine concentration of 25 mg/mL, which is in the range of reported doses in the literature (i.e. 18–35 mg/mL).[39–41] In general, nicotine concentration may vary depending on usage, e-juice, flavouring chemicals, and the e-cig device.[42,43] We chose a basic e-juice composed of 50% propylene glycol and 50% vegetable glycerin (PG/VG) without added flavouring in order to focus on the potential effects of vaped nicotine uptake. Further, nicotine uptake through e-cig vaping is also somewhat dependent on aerosol particle sizes. A recent publication by Lalo et al.,[44] utilizing the same third-generation atomizer as in our experiments and the same mix of PG and VG, but with a slightly lower dose of nicotine (18 mg/mL), found that mass median aerodynamic diameters ranged from 1.06 to 1.19 μm, with nicotine concentrations within the aerosol droplets of approximately

11 mg/mL. These results are consistent with other studies reporting particle sizes within that range.[45,46] The cotinine metabolite levels we achieved in e-cig-exposed mice were consistent with those found in vaping humans.[35] We did not observe significant changes in blood pressure of the mice during a maximum of 6 weeks of e-cig exposure. Notably some other studies have reported increases in murine blood pressure in chronic exposure models, using much longer exposures and lasting up to 60 weeks. However, in one of those studies all significant differences disappeared after 4 weeks.[47,48]

Immune/inflammatory-regulating miRs play a central role in AAA development. A prime example of this is the downregulation of miR-24 in murine AAA models and human tissue, which is regulated in the opposite direction from expression of predicted miR-24-target inflammatory genes in aortic tissue. Nicotine has previously been demonstrated to regulate miR transcription and is capable of altering miR expression systemically as well as locally, with effects that can even be transmitted transgenerationally.[26,49] Here we showed that e-cig exposure in PPE-AAA and AngII/ApoE$^{-/-}$ resulted in further aortic tissue down-regulation of miR-24, accompanied by enhanced up-regulation of inflammatory genes, including its target Chil1, novel findings that connect these key AAA mediators.

Of the two possible miR-24 loci, the one involved in AAA appears to be derived from the intronic miR-24-1-cluster (mouse-chr13; human-chr9: miR-23b/miR-27b/miR-24-1), rather than the intergenic miR-24-2 cluster (mouse-chr8; human-chr19: miR-23a/miR-27a/miR-24-2). The miR-23b-24-27b cluster is highly conserved and has been previously associated with post-infarct cardiac angiogenesis, cardiomyocyte survival, and cancer.[50–53]

We also show *in vitro* that nicotine increases inflammation, and augments the effects of IL-6 in down-regulating pri-miR-24-1 in macrophages and human AoSMCs. Taken together, these data suggest a miR-mediated mechanism for some of nicotine's pathologic effects on aneurysm development.

NF-κB, the core mediator of its namesake AAA-related pathway, mentioned above, can act as a transcriptional repressor, is a well-known mediator of nicotine activity, and can directly regulate miRs.[19,20,54] Looking at potential pathophysiologic mechanisms, we previously established that inflammatory stimuli down-regulate miR-24, at least partly through NF-κB.[29] Our new *in vitro* data suggest that the additional down-regulation of miR-24 observed in macrophages and human AoSMCs with nicotine treatment is also partially mediated by NF-κB. Further, nicotine induced ROS in these cells, and regulation of miR-24-1 by nicotine was dependent on ROS.

While miR-24 regulates numerous genes, our analysis has suggested that one of its targets, CHI3L1/Chil1, is likely crucial in mediating inflammation in AAA.[29] This relatively novel secreted cytokine can induce VSMC proliferation and migration, is a marker of late-stage macrophage differentiation, and is secreted by macrophages *in situ* during atherogenesis.[55] It is thought to contribute to both acute and chronic inflammation.[56–60] Importantly Chil1 has been shown to promote macrophage recruitment in cancer,[61] and promote macrophage polarization towards a pro-inflammatory phenotype,[62,63] which are in line with our *in vivo* and *in vitro* experiments.

In support of these conclusions, we now show that systemic Chil1 knock-out neutralizes the accelerated AAA seen with e-cig exposure in the PPE model, in both genders. Additionally, *in vitro* we show that nicotine augments expression of *CHI3L1/Chil1* in macrophages and human AoSMCs in response to IL6-stimulation, due in part to its effects on miR-24 levels. In fact, nicotine's effects on inflammatory cytokine expression in human AoSMCs *in vitro* appear to be largely dependent on miR-24 and CHI3L1/Chil1.

Finally, paralleling our murine findings, our analysis of human AAA tissue shows that smokers experience greatly decreased miR-24 expression and increased *CHI3L1* expression compared with non-smokers. Since e-cig vaping is currently more frequently employed by younger individuals, and AAA is a chronic disease that typically manifests in the sixth decade of life, insufficient numbers of patients currently exist to evaluate its effects to-date on human AAA risk. Of note, recent evidence demonstrates that e-cig use can negatively affect endothelial function in animal models

and humans, thereby setting the stage for vascular inflammation.[64,65] Our data should therefore serve as a warning of the potentially hazardous impact of e-cigs on AAA incidence in years to come.

Our experiments also highlight the role of gender in AAA development, showing that the response to e-cig elicited in female mice was uniformly less severe than in male mice. This has been noted in several AAA models previously,[66] and reflects human disease incidence.[67,68] AAA-pathophysiology-related gene-regulation was also generally smaller in magnitude in female mice when compared to male mice, including e-cig-induced Chil1. However, it needs to be noted that in both genders Chil1 was shown to be significantly up-regulated in response to nicotine vaping and that Chil1-KO proved to be protective for both genders. A large cohort study found AAA growth in women to be more sensitive to current smoking when compared to men.[69] Our data indicate that Chil1 is a key regulator in nicotine-augmented AAA formation independent of gender. This may also help to explain why the protective effects of female gender are lost in regards to AAA development when active smoking status is considered.[70]

Our study has limitations. First, during our evaluation of experimental AAA growth with vaping we did not perform direct manipulation of miR-24 levels by using (for example) anti- or pre-miR oligonucleotides as in our previous work, but rather decided to focus on one of the major targets of miR-24. It is the case that miR-24 has other targets that may have the potential to alter AAA formation. However, our *in vitro* data suggest that much of the impact of miR-24 regulation on nicotine-induced vascular inflammation is dependent upon Chil1/CHI3L1. Based on our published studies on miR-24/Chil1 in AAA, we would have expected Chil1 deletion to have had a more significant effect in decreasing non-vaped AAA growth, but it appears that a large proportion of the previously observed impact of miR-24 modulation on AAA (independent of nicotine) may relate to complex regulation of its many other targets.[29]

It should also be noted that we did not explore AAA formation in response to exposure to e-cig vapour without nicotine. There is accumulating evidence that the vapourization process produces toxic byproducts that are inhaled and that these may lead to endothelial dysfunction[71] and inflammatory responses,[72,73] and affect vascular function.[74] These effects may have contributed to the observed effects in our *in vivo* model and will be addressed in future studies.

Further, we have included data derived from samples from human patients that smoked conventional cigarettes rather than e-cigs. We are aware of this inconsistency but given the lack of availability of samples from AAA patients with a history of primary e-cig use, at this point there is no other means of accessible clinical validation. Additionally, while these murine models of AAA have been shown in numerous publications to strongly resemble human disease in terms of pathophysiology, they embody a more acute inflammatory process with early rapid AAA growth, as opposed to the more chronic inflammation which dominates human AAA development.

Taken together our data imply that chronic nicotine intake via e-cig vaping may increase AAA risk and progression by augmentation of immune/inflammatory responses via up-regulation of CHI3L1/Chil1 (likely in part due to down-regulation of miR-24). These results add to the growing body of literature suggesting that nicotine-containing products may add to cardiovascular risk in general, and AAA in particular, and raise concerns regarding the potential public health impacts of their chronic use.

Supplementary material

Supplementary material is available at *Cardiovascular Research* online.

Author contributions

Conceptualization: J.M., J.M.S., P.S.T.; Methodology: J.M., J.M.S., P.M., M.U.W.; Investigation: J.M., J.M.S., P.M., M.U.W., A.D., K.T., K.M., Y.H.R., M.A., L.M.; Visualization: J.M., J.M.S., KM; Funding acquisition: J.M.S., L.M., P.S.T.; Project administration: J.M.S., P.S.T.; Supervision: J.M.S., H.S., L.M.,

P.S.T.; Writing—original draft: J.M., J.M.S., P.M., P.S.T.; Writing—review and editing: J.M., J.M.S., P.S.T.

Data availability

The data underlying this article will be shared on reasonable request to the corresponding author.

References

1. Summers KL, Kerut EK, Sheahan CM, Sheahan MG III. Evaluating the prevalence of abdominal aortic aneurysms in the United States through a national screening database. *J Vasc Surg* 2021;**73**:61–68.
2. Schermerhorn ML, Bensley RP, Giles KA, Hurks R, O'Malley AJ, Cotterill P, Chaikof E, Landon BE. Changes in abdominal aortic aneurysm rupture and short-term mortality, 1995-2008: a retrospective observational study. *Ann Surg* 2012;**256**:651–658.
3. Abdulameer H, Al Taii H, Al-Kindi SG, Milner R. Epidemiology of fatal ruptured aortic aneurysms in the United States (1999-2016). *J Vasc Surg* 2019;**69**:378–384 e372.
4. Lederle FA, Nelson DB, Joseph AM. Smokers' relative risk for aortic aneurysm compared with other smoking-related diseases: a systematic review. *J Vasc Surg* 2003;**38**:329–334.
5. Powell JT, Worrell P, MacSweeney ST, Franks PJ, Greenhalgh RM. Smoking as a risk factor for abdominal aortic aneurysm. *Ann N Y Acad Sci* 1996;**800**:246–248.
6. Wilmink TB, Quick CR, Day NE. The association between cigarette smoking and abdominal aortic aneurysms. *J Vasc Surg* 1999;**30**:1099–1105.
7. Buckley C, Wyble CW, Borhani M, Ennis TL, Kobayashi DK, Curci JA, Shapiro SD, Thompson RW. Accelerated enlargement of experimental abdominal aortic aneurysms in a mouse model of chronic cigarette smoke exposure. *J Am Coll Surg* 2004;**199**:896–903.
8. Bergoeing MP, Arif B, Hackmann AE, Ennis TL, Thompson RW, Curci JA. Cigarette smoking increases aortic dilatation without affecting matrix metalloproteinase-9 and -12 expression in a modified mouse model of aneurysm formation. *J Vasc Surg* 2007;**45**:1217–1227.
9. Norman PE, Curci JA. Understanding the effects of tobacco smoke on the pathogenesis of aortic aneurysm. *Arterioscler Thromb Vasc Biol* 2013;**33**:1473–1477.
10. Aune D, Schlesinger S, Norat T, Riboli E. Tobacco smoking and the risk of abdominal aortic aneurysm: a systematic review and meta-analysis of prospective studies. *Sci Rep* 2018;**8**:14786.
11. Bohlin S, Frojd C, Wanhainen A, Bjorck M. Change in smoking habits after having been screened for abdominal aortic aneurysm. *Eur J Vasc Endovasc Surg* 2014;**48**:138–143.
12. Siegel MB, Tanwar KL, Wood KS. Electronic cigarettes as a smoking-cessation: tool results from an online survey. *Am J Prev Med* 2011;**40**:472–475.
13. Moheimani RS, Bhetraratana M, Yin F, Peters KM, Gornbein J, Araujo JA, Middlekauff HR. Increased cardiac sympathetic activity and oxidative stress in habitual electronic cigarette users: implications for cardiovascular risk. *JAMA Cardiol* 2017;**2**:278–284.
14. MacDonald A, Middlekauff HR. Electronic cigarettes and cardiovascular health: what do we know so far? *Vasc Health Risk Manag* 2019;**15**:159–174.
15. Alzahrani T, Glantz SA. Adding data from 2015 strengthens the association between E-cigarette use and myocardial infarction. *Am J Prev Med* 2019;**57**:569–571.
16. Geiss O, Bianchi I, Barahona F, Barrero-Moreno J. Characterisation of mainstream and passive vapours emitted by selected electronic cigarettes. *Int J Hyg Environ Health* 2015;**218**:169–180.

17. Lee WH, Ong SG, Zhou Y, Tian L, Bae HR, Baker N, Whitlatch A, Mohammadi L, Guo H, Nadeau KC, Springer ML, Schick SF, Bhatnagar A, Wu JC. Modeling cardiovascular risks of E-cigarettes with human-induced pluripotent stem cell-derived endothelial cells. *J Am Coll Cardiol* 2019;**73**:2722–2737.

18. Marsot A, Simon N. Nicotine and cotinine levels with electronic cigarette: a review. *Int J Toxicol* 2016;**35**:179–185.

19. Lau PP, Li L, Merched AJ, Zhang AL, Ko KW, Chan L. Nicotine induces proinflammatory responses in macrophages and the aorta leading to acceleration of atherosclerosis in low-density lipoprotein receptor(-/-) mice. *Arterioscler Thromb Vasc Biol* 2006;**26**:143–149.

20. Maegdefessel L, Azuma J, Toh R, Deng A, Merk DR, Raiesdana A, Leeper NJ, Raaz U, Schoelmerich AM, McConnell MV, Dalman RL, Spin JM, Tsao PS. MicroRNA-21 blocks abdominal aortic aneurysm development and nicotine-augmented expansion. *Sci Transl Med* 2012;**4**:122ra122.

21. Wang S, Zhang C, Zhang M, Liang B, Zhu H, Lee J, Viollet B, Xia L, Zhang Y, Zou MH. Activation of AMP-activated protein kinase alpha2 by nicotine instigates formation of abdominal aortic aneurysms in mice in vivo. *Nat Med* 2012;**18**:902–910.

22. Raaz U, Zollner AM, Schellinger IN, Toh R, Nakagami F, Brandt M, Emrich FC, Kayama Y, Eken S, Adam M, Maegdefessel L, Hertel T, Deng A, Jagger A, Buerke M, Dalman RL, Spin JM, Kuhl E, Tsao PS. Segmental aortic stiffening contributes to experimental abdominal aortic aneurysm development. *Circulation* 2015;**131**:1783–1795.

23. Wagenhauser MU, Schellinger IN, Yoshino T, Toyama K, Kayama Y, Deng A, Guenther SP, Petzold A, Mulorz J, Mulorz P, Hasenfuss G, Ibing W, Elvers M, Schuster A, Ramasubramanian AK, Adam M, Schelzig H, Spin JM, Raaz U, Tsao PS. Chronic nicotine exposure induces murine aortic remodeling and stiffness segmentation-implications for abdominal aortic aneurysm susceptibility. *Front Physiol* 2018;**9**:1459.

24. Pillai RS, Bhattacharyya SN, Filipowicz W. Repression of protein synthesis by miRNAs: how many mechanisms? *Trends Cell Biol* 2007;**17**:118–126.

25. Ng TK, Carballosa CM, Pelaez D, Wong HK, Choy KW, Pang CP, Cheung HS. Nicotine alters microRNA expression and hinders human adult stem cell regenerative potential. *Stem Cells Dev* 2013;**22**:781–790.

26. Taki FA, Pan X, Zhang B. Chronic nicotine exposure systemically alters microRNA expression profiles during post-embryonic stages in Caenorhabditis elegans. *J Cell Physiol* 2014;**229**:79–89.

27. Merk DR, Chin JT, Dake BA, Maegdefessel L, Miller MO, Kimura N, Tsao PS, Iosef C, Berry GJ, Mohr FW, Spin JM, Alvira LM, Robbins RC, Fischbein MP. miR-29b participates in early aneurysm development in Marfan syndrome. *Circ Res* 2012;**110**:312–324.

28. Maegdefessel L, Azuma J, Toh R, Merk DR, Deng A, Chin JT, Raaz U, Schoelmerich AM, Raiesdana A, Leeper NJ, McConnell MV, Dalman RL, Spin JM, Tsao PS. Inhibition of microRNA-29b reduces murine abdominal aortic aneurysm development. *J Clin Invest* 2012;**122**:497–506.

29. Maegdefessel L, Spin JM, Raaz U, Eken SM, Toh R, Azuma J, Adam M, Nagakami F, Heymann HM, Chernugobova E, Jin H, Roy J, Hultgren R, Caidahl K, Schrepfer S, Hamsten A, Eriksson P, McConnell MV, Dalman RL, Tsao PS. miR-24 limits aortic vascular inflammation and murine abdominal aneurysm development. *Nat Commun* 2014;**5**:5214.

30. Kastrup J. Can YKL-40 be a new inflammatory biomarker in cardiovascular disease? *Immunobiology* 2012;**217**:483–491.

31. Azuma J, Asagami T, Dalman R, Tsao PS. Creation of murine experimental abdominal aortic aneurysms with elastase. *J Vis Exp* 2009;**29**:1280.

32. Goergen CJ, Azuma J, Barr KN, Magdefessel L, Kallop DY, Gogineni A, Grewall A, Weimer RM, Connolly AJ, Dalman RL, Taylor CA, Tsao PS, Greve JM. Influences of aortic motion and curvature on vessel expansion in murine experimental aneurysms. *Arterioscler Thromb Vasc Biol* 2011;**31**:270–279.

33. Feng J, Whitesall S, Zhang Y, Beibel M, D'Alecy L, DiPetrillo K. Validation of volume-pressure recording tail-cuff blood pressure measurements. *Am J Hypertens* 2008;**21**:1288–1291.

34. Schindelin J, Arganda-Carreras I, Frise E, Kaynig V, Longair M, Pietzsch T, Preibisch S, Rueden C, Saalfeld S, Schmid B, Tinevez JY, White DJ, Hartenstein V, Eliceiri K, Tomancak P, Cardona A. Fiji: an open-source platform for biological-image analysis. *Nat Methods* 2012;**9**:676–682.

35. Flouris AD, Chorti MS, Poulianiti KP, Jamurtas AZ, Kostikas K, Tzatzarakis MN, Wallace Hayes A, Tsatsakis AM, Koutedakis Y. Acute impact of active and passive electronic cigarette smoking on serum cotinine and lung function. *Inhal Toxicol* 2013;**25**:91–101.

36. Raaz U, Toh R, Maegdefessel L, Adam M, Nakagami F, Emrich FC, Spin JM, Tsao PS. Hemodynamic regulation of reactive oxygen species: implications for vascular diseases. *Antioxid Redox Signal* 2014;**20**:914–928.

37. Wang S, Desai D, Wright G, Niles RM, Wright GL. Effects of protein kinase C alpha over-expression on A7r5 smooth muscle cell proliferation and differentiation. *Exp Cell Res* 1997;**236**:117–126.

38. Powell JT, Greenhalgh RM. Clinical practice. Small abdominal aortic aneurysms. *N Engl J Med* 2003;**348**:1895–1901.

39. Lopez AA, Hiler MM, Soule EK, Ramoa CP, Karaoghlanian NV, Lipato T, Breland AB, Shihadeh AL, Eissenberg T. Effects of electronic cigarette liquid nicotine concentration on plasma nicotine and puff topography in tobacco cigarette smokers: a preliminary report. *Nicotine Tob Res* 2016;**18**:720–723.

40. Dawkins LE, Kimber CF, Doig M, Feyerabend C, Corcoran O. Self-titration by experienced e-cigarette users: blood nicotine delivery and subjective effects. *Psychopharmacology (Berl)* 2016;**233**:2933–2941.

41. Raymond BH, Collette-Merrill K, Harrison RG, Jarvis S, Rasmussen RJ. The nicotine content of a sample of E-cigarette liquid manufactured in the United States. *J Addict Med* 2018;**12**:127–131.

42. DeVito EE, Krishnan-Sarin S. E-cigarettes: impact of E-liquid components and device characteristics on nicotine exposure. *Curr Neuropharmacol* 2018;**16**:438–459.

43. El-Hellani A, Salman R, El-Hage R, Talih S, Malek N, Baalbaki R, Karaoghlanian N, Nakkash R, Shihadeh A, Saliba NA. Nicotine and carbonyl emissions from popular electronic cigarette products: correlation to liquid composition and design characteristics. *Nicotine Tob Res* 2018;**20**:215–223.

44. Lalo H, Leclerc L, Sorin J, Pourchez J. Aerosol droplet-size distribution and airborne nicotine portioning in particle and gas phases emitted by electronic cigarettes. *Sci Rep* 2020;**10**:21707.

45. Mulder HA, Patterson JL, Halquist MS, Kosmider L, Turner JBM, Poklis JL, Poklis A, Peace MR. The effect of electronic cigarette user modifications and E-liquid adulteration on the particle size profile of an aerosolized product. *Sci Rep* 2019;**9**:10221.

46. Zhang Y, Sumner W, Chen DR. In vitro particle size distributions in electronic and conventional cigarette aerosols suggest comparable deposition patterns. *Nicotine Tob Res* 2013;**15**:501–508.

47. Crotty Alexander LE, Drummond CA, Hepokoski M, Mathew D, Moshensky A, Willeford A, Das S, Singh P, Yong Z, Lee JH, Vega K, Du A, Shin J, Javier C, Tian J, Brown JH, Breen EC. Chronic inhalation of e-cigarette vapor containing nicotine disrupts airway barrier function and induces systemic inflammation and multiorgan fibrosis in mice. *Am J Physiol Regul Integr Comp Physiol* 2018;**314**:R834–R847.

48. El-Mahdy MA, Ewees MG, Eid MS, Mahgoup EM, Khaleel SA, Zweier JL. Electronic cigarette exposure causes vascular endothelial dysfunction due to NADPH oxidase activation and eNOS uncoupling. *Am J Physiol Heart Circ Physiol* 2022;**322**:H549–H567.

49. Taki FA, Pan X, Lee MH, Zhang B. Nicotine exposure and transgenerational impact: a prospective study on small regulatory microRNAs. *Sci Rep* 2014;**4**:7513.

50. Wang T, Zhang X, Obijuru L, Laser J, Aris V, Lee P, Mittal K, Soteropoulos P, Wei JJ. A micro-RNA signature associated with race, tumor size, and target gene activity in human uterine leiomyomas. *Genes Chromosomes Cancer* 2007;**46**:336–347.

51. Fiedler J, Jazbutyte V, Kirchmaier BC, Gupta SK, Lorenzen J, Hartmann D, Galuppo P, Kneitz S, Pena JT, Sohn-Lee C, Loyer X, Soutschek J, Brand T, Tuschl T, Heineke J, Martin U, Schulte-Merker S, Ertl G, Engelhardt S, Bauersachs J, Thum T. MicroRNA-24 regulates vascularity after myocardial infarction. *Circulation* 2011;**124**:720–730.

52. Melkman-Zehavi T, Oren R, Kredo-Russo S, Shapira T, Mandelbaum AD, Rivkin N, Nir T, Lennox KA, Behlke MA, Dor Y, Hornstein E. miRNAs control insulin content in pancreatic beta-cells via downregulation of transcriptional repressors. *EMBO J* 2011;**30**:835–845.

53. Qian L, Van Laake LW, Huang Y, Liu S, Wendland MF, Srivastava D. miR-24 inhibits apoptosis and represses bim in mouse cardiomyocytes. *J Exp Med* 2011;**208**:549–560.

54. Baetz D, Regula KM, Ens K, Shaw J, Kothari S, Yurkova N, Kirshenbaum LA. Nuclear factor-kappaB-mediated cell survival involves transcriptional silencing of the mitochondrial death gene BNIP3 in ventricular myocytes. *Circulation* 2005;**112**:3777–3785.

55. Zhao T, Su Z, Li Y, Zhang X, You Q. Chitinase-3 like-protein-1 function and its role in diseases. *Signal Transduct Target Ther* 2020;**5**:201.

56. Volck B, Price PA, Johansen JS, Sorensen O, Benfield TL, Nielsen HJ, Calafat J, Borregaard N. YKL-40, a mammalian member of the chitinase family, is a matrix protein of specific granules in human neutrophils. *Proc Assoc Am Physicians* 1998;**110**:351–360.

57. Boot RG, van Achterberg TA, van Aken BE, Renkema GH, Jacobs MJ, Aerts JM, de Vries CJ. Strong induction of members of the chitinase family of proteins in atherosclerosis: chitotriosidase and human cartilage gp-39 expressed in lesion macrophages. *Arterioscler Thromb Vasc Biol* 1999;**19**:687–694.

58. Vos K, Steenbakkers P, Miltenburg AM, Bos E, van Den Heuvel MW, van Hogezand RA, de Vries RR, Breedveld FC, Boots AM. Raised human cartilage glycoprotein-39 plasma levels in patients with rheumatoid arthritis and other inflammatory conditions. *Ann Rheum Dis* 2000;**59**:544–548.

59. Nishikawa KC, Millis AJ. Gp38k (CHI3L1) is a novel adhesion and migration factor for vascular cells. *Exp Cell Res* 2003;**287**:79–87.

60. Rehli M, Niller HH, Ammon C, Langmann S, Schwarzfischer L, Andreesen R, Krause SW. Transcriptional regulation of CHI3L1, a marker gene for late stages of macrophage differentiation. *J Biol Chem* 2003;**278**:44058–44067.

61. Kawada M, Seno H, Kanda K, Nakanishi Y, Akitake R, Komekado H, Kawada K, Sakai Y, Mizoguchi E, Chiba T. Chitinase 3-like 1 promotes macrophage recruitment and angiogenesis in colorectal cancer. *Oncogene* 2012;**31**:3111–3123.

62. Kim MJ, Shim DH, Cha HR, Moon KY, Yang CM, Hwang SJ, Kim KW, Park JH, Lee CG, Elias JA, Sohn MH, Lee JM. Chitinase 3-like 1 protein plays a critical role in respiratory syncytial virus-induced airway inflammation. *Allergy* 2019;**74**:685–697.

63. Xu N, Bo Q, Shao R, Liang J, Zhai Y, Yang S, Wang F, Sun X. Chitinase-3-Like-1 promotes M2 macrophage differentiation and induces choroidal neovascularization in neovascular age-related macular degeneration. *Invest Ophthalmol Vis Sci* 2019;**60**:4596–4605.

64. El-Mahdy MA, Mahgoup EM, Ewees MG, Eid MS, Abdelghany TM, Zweier JL. Long-Term electronic cigarette exposure induces cardiovascular dysfunction similar to tobacco cigarettes: role of nicotine and exposure duration. *Am J Physiol Heart Circ Physiol* 2021;**320**:H2112–H2129.

65. Whitehead AK, Erwin AP, Yue X. Nicotine and vascular dysfunction. *Acta Physiol (Oxf)* 2021;**231**:e13631.

66. DiMusto PD, Lu G, Ghosh A, Roelofs KJ, Sadiq O, McEvoy B, Su G, Laser A, Bhamidipati CM, Ailawadi G, Henke PK, Eliason JL, Upchurch GR Jr. Increased JNK in males compared with females in a rodent model of abdominal aortic aneurysm. *J Surg Res* 2012;**176**:687–695.

67. Hannawa KK, Eliason JL, Upchurch GR. Gender differences in abdominal aortic aneurysms. *Vascular* 2009;**17**(Suppl 1):S30–S39.

68. Villard C, Hultgren R. Abdominal aortic aneurysm: sex differences. *Maturitas* 2018;**109**: 63–69.

69. Stackelberg O, Bjorck M, Larsson SC, Orsini N, Wolk A. Sex differences in the association between smoking and abdominal aortic aneurysm. *Br J Surg* 2014;**101**:1230–1237.

70. Carter JL, Morris DR, Sherliker P, Clack R, Lam KBH, Halliday A, Clarke R, Lewington S, Bulbulia R. Sex-Specific associations of vascular risk factors with abdominal aortic aneurysm: findings from 1.5 million women and 0.8 million men in the United States and United Kingdom. *J Am Heart Assoc* 2020;**9**:e014748.

71. Kuntic M, Oelze M, Steven S, Kroller-Schon S, Stamm P, Kalinovic S, Frenis K, Vujacic-Mirski K, Bayo Jimenez MT, Kvandova M, Filippou K, Al Zuabi A, Bruckl V, Hahad O, Daub S, Varveri F, Gori T, Huesmann R, Hoffmann T, Schmidt FP, Keaney JF, Daiber A, Munzel T. Short-term e-cigarette vapour exposure causes vascular oxidative stress and dysfunction: evidence for a close connection to brain damage and a key role of the phagocytic NADPH oxidase (NOX-2). *Eur Heart J* 2020;**41**:2472–2483.

72. Gellatly S, Pavelka N, Crue T, Schweitzer KS, Day BJ, Min E, Numata M, Voelker DR, Scruggs A, Petrache I, Chu HW. Nicotine-Free e-cigarette vapor exposure stimulates IL6 and mucin production in human primary small airway epithelial cells. *J Inflamm Res* 2020;**13**:175–185.

73. Chatterjee S, Tao JQ, Johncola A, Guo W, Caporale A, Langham MC, Wehrli FW. Acute exposure to e-cigarettes causes inflammation and pulmonary endothelial oxidative stress in nonsmoking, healthy young subjects. *Am J Physiol Lung Cell Mol Physiol* 2019;**317**: L155–L166.

74. Caporale A, Langham MC, Guo W, Johncola A, Chatterjee S, Wehrli FW. Acute effects of electronic cigarette aerosol inhalation on vascular function detected at quantitative MRI. *Radiology* 2019;**293**:97–106.

Translational perspective

Smoking is one of the most hazardous modifiable risk factors, with clear links to abdominal aortic aneurysm. E-cig vaping has displayed explosive growth in popularity. Intended for smoking cessation, it has been taken up by millions with no such clinical need, delivering nicotine addiction to new generations. The presumption that vaping is safer than tobacco overlooks the potential cardiovascular risks of nicotine. This study shows for the first time that inhaled e-cig nicotine vapour augments experimental AAA and aortic inflammation, suggests a mechanistic role for the cytokine Chil1/CHI3L1 and its regulator microRNA-24, and raises red flags regarding longitudinal e-cig safety.